Supporting Information

Modification of graphene oxide/$V_2O_5 \bullet nH_2O$ nanocomposite films via direct laser irradiation

Algirdas Lazauskas[a, b]*, *Liutauras Marcinauskas*[a, c], *Mindaugas Andrulevicius*[b]

[a] Plasma Processing Laboratory, Lithuanian Energy Institute, Breslaujos 3, LT44403 Kaunas, Lithuania

[b] Institute of Materials Science, Kaunas University of Technology, K. Baršausko 59, LT51423 Kaunas, Lithuania

[c] Department of Physics, Kaunas University of Technology, Studentų 50, LT-51368 Kaunas, Lithuania

***Corresponding Author**

Algirdas Lazauskas

Telephone: + 370-671-73375

Email: algirdas.lazauskas@ktu.lt

MATERIALS AND METHODS

Formation of GO/V_2O_5•*n*H_2O nanocomposite films. The V_2O_5•*n*H_2O was prepared via melt-quenching process. Briefly, 10 g of crystalline V_2O_5 powder taken in a ceramic crucible was heated to 750 °C in a muffle furnace for 50 min. The resulting molten V_2O_5 liquid was quickly poured into deionized water with stirring and sonicated for 30 min. The brownish V_2O_5•*n*H_2O was obtained by filtering and drying the suspension. The GO synthesis was performed via modified Hummer's method as reported in [44]. Herein, instead of ultrasonication the mechanical stirring method with conventional blender was used to suspend GO flakes in water (concentration – 5 mg/ml). Afterwards, 15 ml of this suspension was mixed with 5 ml of V_2O_5•*n*H_2O (concentration – 12 mg/ml). We used the final mixture to deposit GO/V_2O_5•*n*H_2O nanocomposite films on (1 0 0) GaAs and glass substrates via drop-casting method. The films were left to dry in a vacuum drying oven Vacucentre VC50 (SalvisLab) at a temperature of 35 °C and pressure of 400 mbar. After drying, samples for photothermal reduction experiments were obtained.

Photothermal modification of GO/V_2O_5•*n*H_2O nanocomposite films. Direct laser irradiation experiments were performed using a simple laser system using a compact and low-cost blue-violet CW semiconductor laser (rated power of 500 mW and a wavelength of 405 nm) with adjustable focal length and pulse width modulation (PWM) input (analog). Laser irradiation process was conducted following the black rectangle pattern controlled by a computer program. Laser power density was varied in the range of 1.69–2.71 × 10^5 W/cm^2 while writing speed remained constant at 0.3 mm/s. Direct laser irradiation experiments were performed in air under ambient conditions.

Characterization. A transmission electron microscope (TEM) Tecnai G2 F20 X-TWIN was used to examine as-prepared $V_2O_5 \bullet nH_2O$, GO flakes and GO/$V_2O_5 \bullet nH_2O$. The accelerating voltage was 200 kV. The crystallographic nature of the powder samples was determined using D8 Discover X-ray diffractometer (Bruker AXS GmbH) with Cu K_α (λ= 1.54 Å) X-ray source. Parallel beam geometry with 60 mm Göbel mirror (i.e. X-ray mirror on a high precision parabolic surface) was used. This configuration enables transforming the divergent incident X-ray beam from a line focus of the X-ray tube into a parallel beam that is free of K_β radiation. Primary side also had a Soller slit with an axial divergence of 2.5 º. The secondary side had a LYNXEYE (0D mode) detector with an opening angle of 2.475 º and slit opening of 9.5 mm. X-ray generator voltage and current was 40.0 kV and 40 mA, respectively. Coupled 2θ/θ scans were performed in the range of 3.0-130.0 º with a step size of 0.064 º, time per step of 19.2 s and auto-repeat function enabled. Processing of the resultant diffractograms was performed with DIFFRAC.EVA software. Powder refinement procedures were performed with expo v1.14.10 program for automatic solution of crystal structures.[1] The non-structural parameters were refined with Le Bail method; background was described with Chebyshev polynomial function, while the Pearson VII was used as a peak shape function.[2] For the X-ray diffraction measurements at grazing incidence (XRDGI) the detector opening angle was set to 1.275° and slit opening on the secondary side to 9.5 mm. The XRDGI scans were performed at incidence angle of 1.50°, in the range of 3.0–134.0° with a step size of 0.065°, time per step of 0.1 s and auto-repeat function enabled. Surface morphology of the resulting GO/$V_2O_5 \bullet nH_2O$ and rGO/$V_2O_5 \bullet nH_2O$ nanocomposite films was investigated using SEM. The SEM micrographs were acquired using S-3400N SEM instrument (Hitachi). Quantitative analysis of surface features was performed with ilastik software, version 1.3.2, for supervised pixel- and object-level classification.[3] The

specific surface area measured by N_2 adsorption employing Kelvin 1042 sorptometer (Costech Instruments) and calculated utilizing the Brunauer-Emett-Teller (BET) method. The sample was degassed under vacuum (0.1 mmHg) at 150 °C for 3 h prior to the surface area determination. Raman spectra were recorded using inVia Raman spectrometer (Renishaw) equipped with CCD camera and confocal microscope (50× objective). The Raman spectra were excited with 532 nm radiation of semiconductor green laser at 5% output power in order to avoid damage of the sample. The 2400 lines/mm grating was used to record the Raman spectra (10 × 10 s accumulation time). Parameters of the GO and rGO bands were determined by fitting the experimental spectra with Gaussian shape components using OriginPro 8.0 (OriginLab) software. Current–voltage (I–V) characteristics of GO/V_2O_5•$n$$H_2O$ and rGO/V_2O_5•$n$$H_2O$ nanocomposite films were measured using a picoammeter/voltage source Keithley 6487. XPS was performed for surface chemical analysis of crystalline V_2O_5, V_2O_5•$n$$H_2O$, GO, GO/$V_2O_5$•$n$$H_2O$ and rGO/V_2O_5•$n$$H_2O$. The Thermo Scientific ESCALAB 250Xi spectrometer with monochromatized Al Kα radiation (hν=1486.6 eV) was used in this study. The diameter of X-Ray spot was 0.9 mm. The base pressure in the analytical chamber was better than 3 x 10^{-9} Torr. The hemispherical electron energy analyzer was used for spectra acquisition, operating in Fixed Analyzer Transmission mode and 40 eV pass energy. Energy scale of the system was calibrated according to Au $4f_{7/2}$, Ag $3d_{5/2}$ and Cu $2p_{3/2}$ peaks position. Peak fitting procedure was performed using original ESCALAB 250Xi Avantage software. The samples were analyzed as received, without additional preparation.

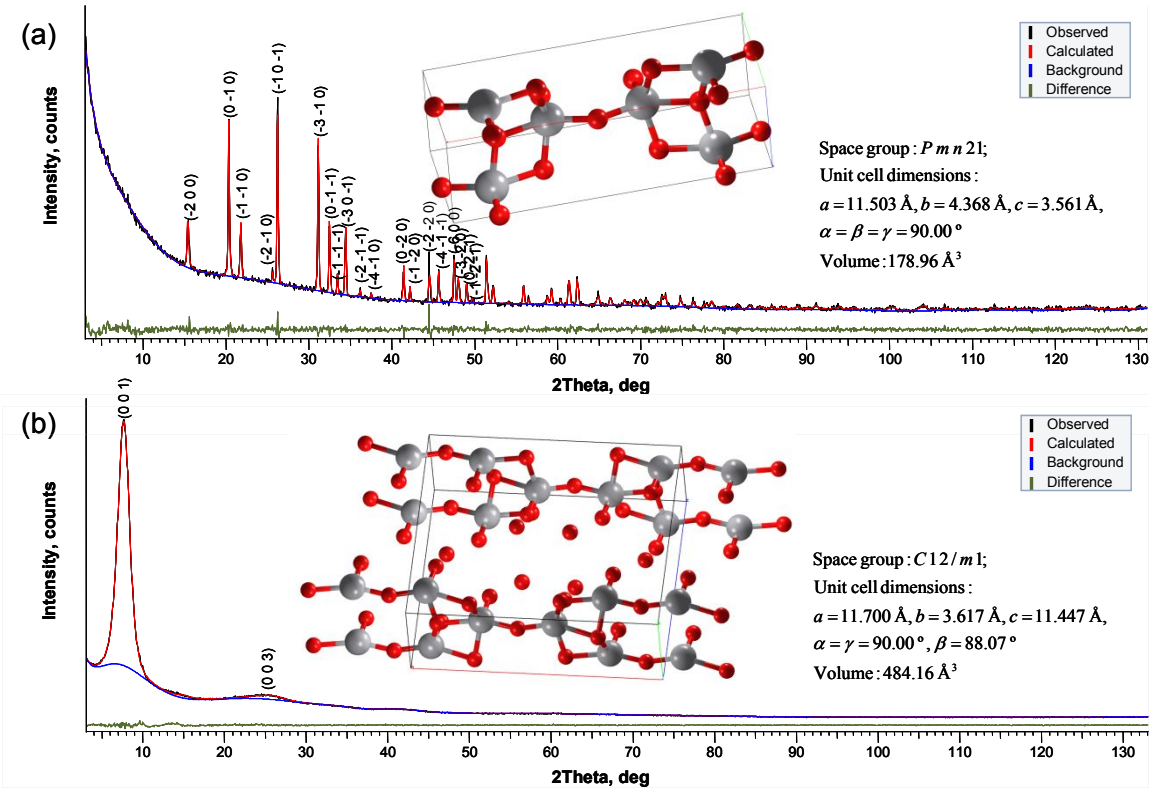

Figure S1. Experimental and calculated XRD patterns with background line and difference of (a) crystalline V_2O_5 (space group *P m n* 21) and (b) V_2O_5•nH_2O (space group space group *C* 1 2/*m* 1) unit cells with crystallographic plane orientations indicated; insets show crystal structure visualizations and the main parameters of unit cells, respectively.

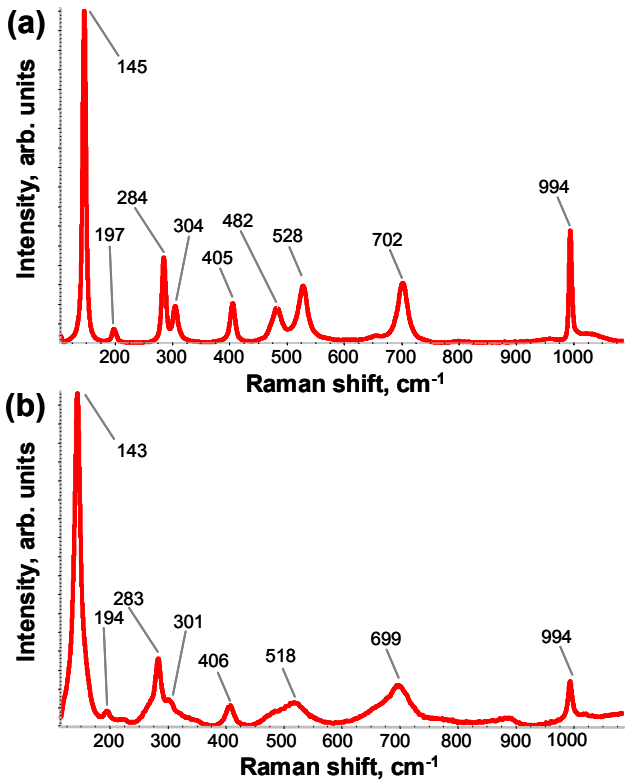

Figure S2. Raman spectra of (a) crystalline V_2O_5 and (b) $V_2O_5 \bullet nH_2O$ recorded at 532 nm excitation wavelength.

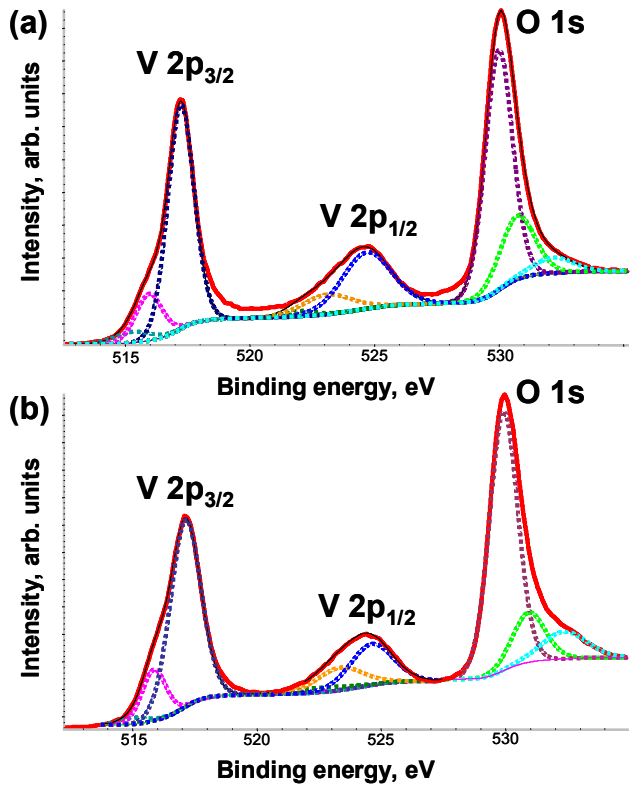

Figure S3. Deconvoluted high-resolution XPS V 2p and O 1s spectra of (a) crystalline V_2O_5 and (b) V_2O_5•nH_2O. Thick red lines – experimental data, thin black lines – envelope, thick dashed lines – fitted components.

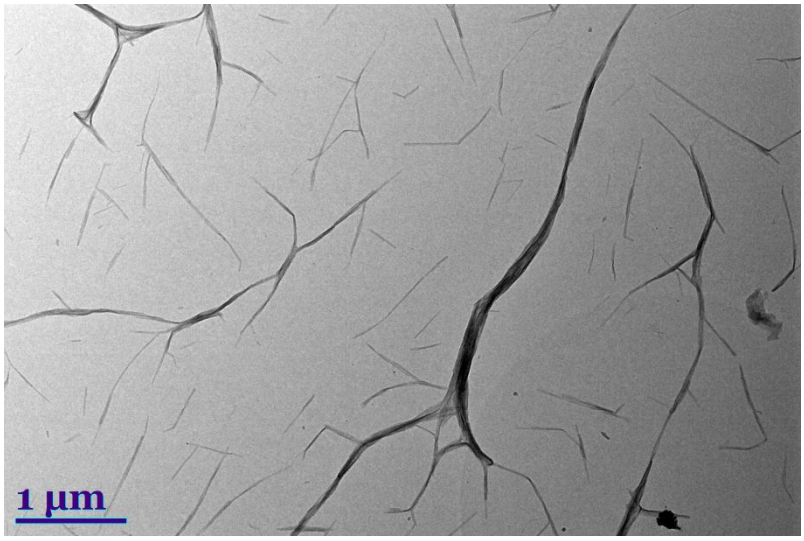

Figure S4. TEM micrograph of V_2O_5•nH_2O nanoribbons.

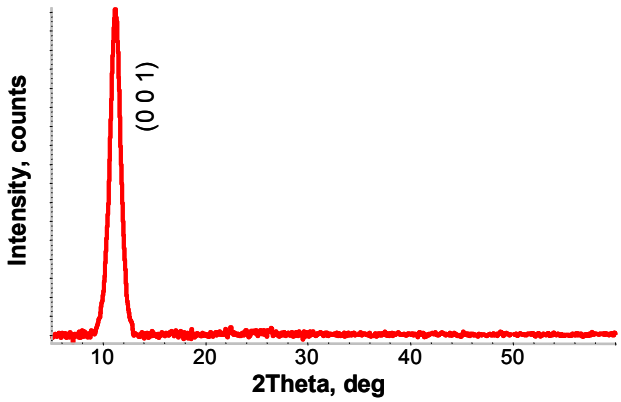

Figure. S5. XRD pattern of GO with crystallographic plane orientation indicated.

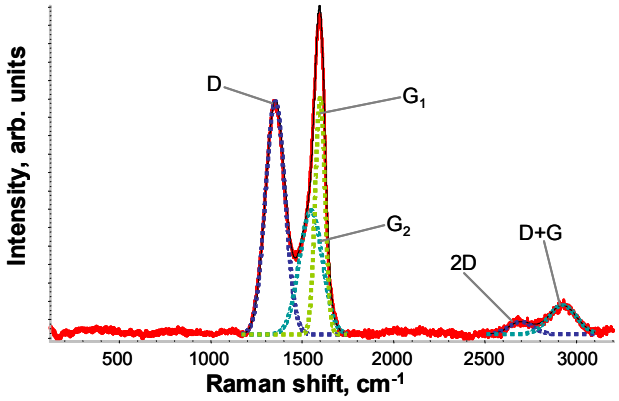

Figure S6. Raman spectrum of GO with deconvoluted bands using Gaussian components. Thick red lines present acquired data; thin black lines – envelope, thick dashed lines – fitted components.

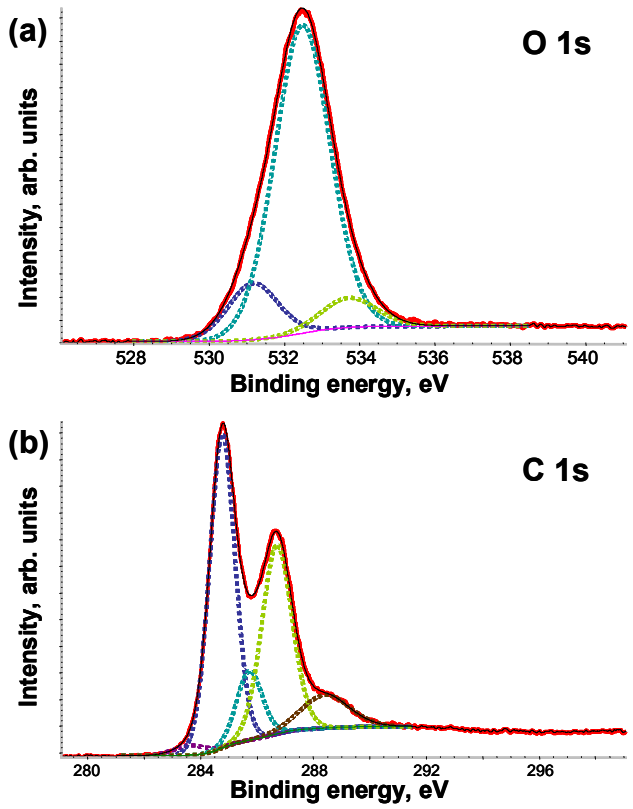

Figure S7. Deconvoluted high-resolution XPS (a) O 1s and (b) C 1s spectra of GO. Thick red lines – experimental data, thin black lines – envelope, thick dashed lines – fitted components.

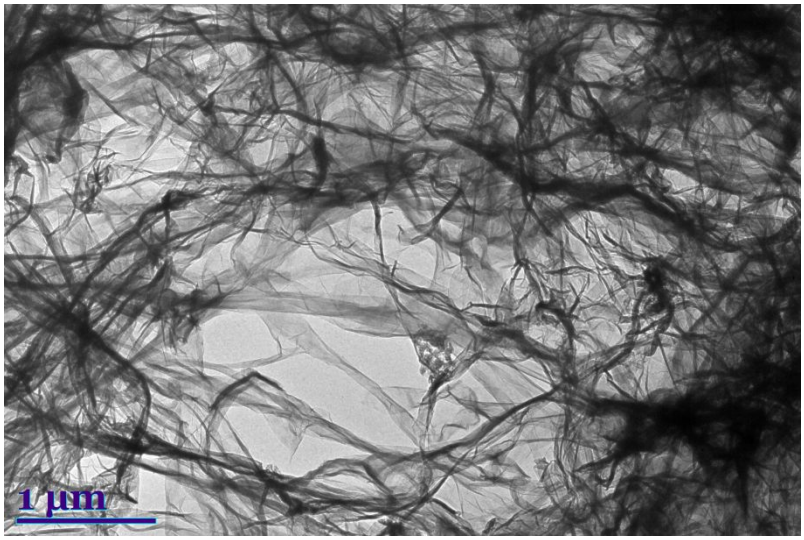

Figure S8. TEM micrograph of GO flakes.

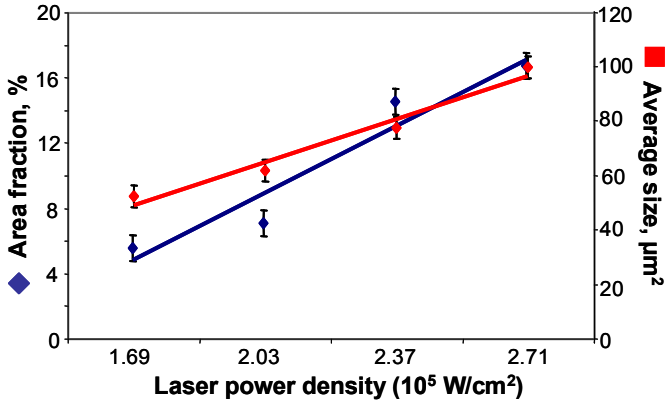

Figure S9. Cluster formation dependence on laser power density. R^2 for trend lines ≥ 0.92.

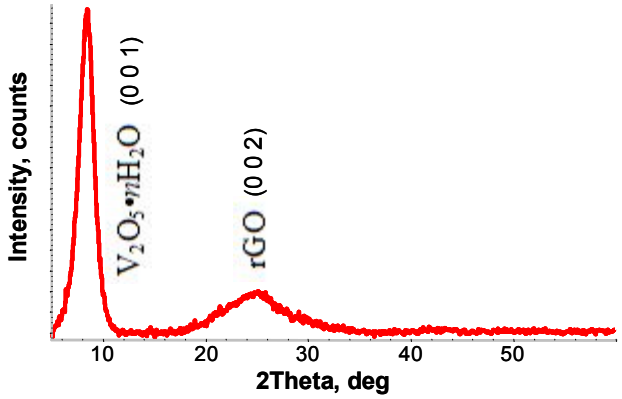

Figure S10. Characteristic XRDGI pattern of rGO/V_2O_5•nH_2O nanocomposite film with crystallographic plane orientations indicated.

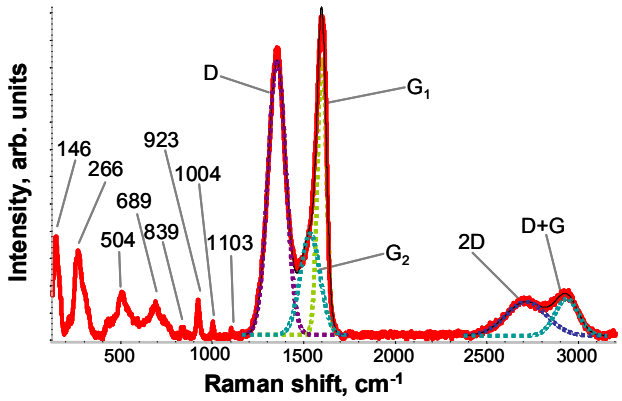

Figure S11. Characteristic Raman spectrum of rGO/V_2O_5•nH_2O nanocomposite film. Deconvoluted bands using Gaussian components for rGO: thick red lines - experimental data; thin black lines – envelope, thick dashed lines – fitted components.

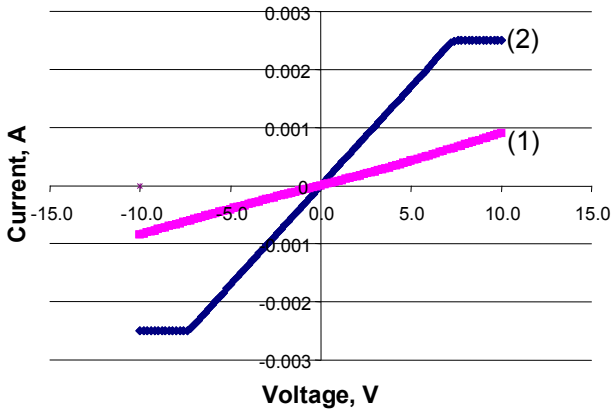

Figure S12. I-V curves of (1) GO/V_2O_5•nH_2O and (2) rGO/V_2O_5•nH_2O nanocomposite films.

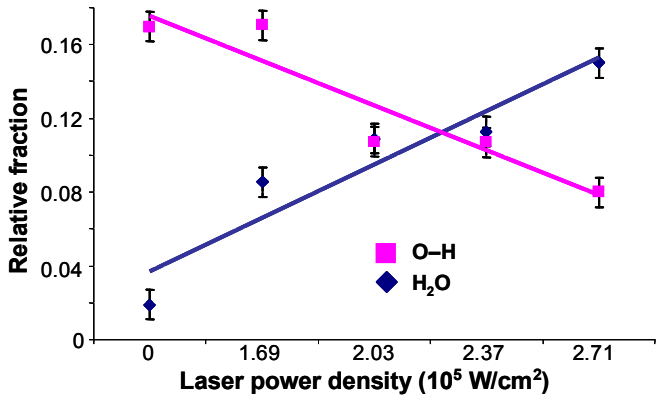

Figure S13. Evolution of water molecules and changes in O–H groups depending on laser power density for rGO/V_2O_5•$n$$H_2O$ nanocomposite films. R^2 for trend lines ≥ 0.87.

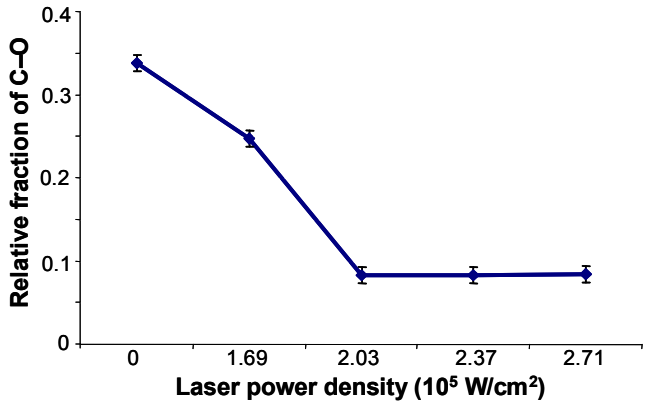

Figure S14. The C–O chemical bond changes depending on the laser power density for rGO/V_2O_5•$n$$H_2O$ nanocomposite films.

SUPPORTING REFERENCES

1. Altomare, A.; Cuocci, C.; Giacovazzo, C.; Moliterni, A.; Rizzi, R.; Corriero, N.; Falcicchio, A., EXPO2013: a kit of tools for phasing crystal structures from powder data. *J. Appl. Crystallogr.* **2013,** *46* (4), 1231-1235.

2. McCusker, L.; Von Dreele, R.; Cox, D.; Louër, D.; Scardi, P., Rietveld refinement guidelines. *J. Appl. Crystallogr.* **1999,** *32* (1), 36-50.

3. Sommer, C.; Straehle, C.; Koethe, U.; Hamprecht, F. A. In *Ilastik: Interactive learning and segmentation toolkit*, 2011 IEEE international symposium on biomedical imaging: From nano to macro, IEEE: **2011**; pp 230-233.